Temperature-dependent ultracold neutron transmission in $^2H_2$ gas: A test of the Young-Koppel model

G. Bison [1], R. Grössle [2,*], K. Kirch [1,3], B. Lauss [1], F. Priester [2], I. Rienäcker [1], and G. Zsigmond [1,†]

[1] *Laboratory for Particle Physics, PSI Center for Neutron and Muon Sciences, Paul Scherrer Institute, Forschungsstrasse 111, 5232 Villigen PSI, Switzerland*

[2] *KIT - Karlsruhe Institute of Technology, DE-76187 Karlsruhe, Germany*

[3] *Institute for Particle Physics and Astrophysics, ETHZ, 8093 Zurich, Switzerland*

(Received 16 October 2024; accepted 10 June 2025; published 21 July 2025)

The Young-Koppel (YK) model describes comprehensively the interaction of slow neutrons with diatomic gases such as H_2 and $^2H_2$. This paper reports on the first experimental results of ultracold neutron (UCN) scattering over a wide temperature range vindicating the YK model for gaseous $^2H_2$ and showing an important difference in the temperature dependence to a low-energy low-temperature approximation (LETA). LETA is confirmed, however, to be valid for monoatomic gases such as Ne. Calculated cross sections for other noble gases were also confirmed for ultracold neutrons. Finally, the total cross section of UCNs in H_2 gas was measured and analyzed applying the Young-Koppel model, however, in a more limited temperature range, confirming the theoretical prediction.

DOI: 10.1103/1r5v-6h9p

I. INTRODUCTION

Ultracold neutrons (UCN) are free neutrons with kinetic energies below about 300 neV that experience total reflection under all angles of incidence from surfaces of suitable materials [1]. The UCN source at the Paul Scherrer Institute [2–4] is used for various fundamental particle physics experiments, such as the search for an electric dipole moment of the neutron [5,6] and a measurement of the free neutron lifetime [7].

The present work investigates the interaction between slow neutrons and individual deuterium molecules. This interaction, by its fundamental nature, has intrigued researchers from the early days of neutron physics [8–10] and remains highly topical until today in nuclear physics, for example, in high-precision measurements of the hadronic interaction [11,12] and in the design of neutron sources [13,14]. It also has important practical implications for the nonstandard operating conditions of the PSI UCN source when considerable $^2H_2$, referred to later as D_2, vapor pressure is present above the solid D_2 [15], as UCN-D_2 scattering can lead to significant UCN losses via up scattering, i.e., neutrons acquire large enough energies to leave the UCN energy range.

In this work we tested the Young-Koppel model [16] that can be applied to describe the interaction between UCNs and H_2 or D_2 gases. It is the first time that the Young-Koppel model was tested over a wide temperature range from about 100 K to above 300 K. The temperature dependence is its unique signature for distinguishing it from the monoatomic approximation.

II. THEORETICAL DESCRIPTION

Young and Koppel (YK) calculated the neutron scattering cross sections from hydrogen and deuterium molecules by taking into consideration the spin correlation effects, as well as rotation and vibration of the molecules [16,17]. In this approach, they considered vibrations as harmonic and decoupled from rotation. Also, there is no interaction between the molecules, which would be the case in high-pressure gases or in liquids. The YK model can also be applied for liquids, however, for incident neutrons with energies less than roughly the solid-state Debye temperature it is not accurate [16]. When the YK model was published, it was supported only by a limited amount of experimental data of the total cross section of neutrons in hydrogen gas as a function of incident energy [18].

Later, the hydrogen gas form factor was measured as a function of scattering angle with inelastic neutron scattering [19]. An excellent match was obtained with the YK model predictions, however, only in a very limited parameter space, at 18 K and one incident energy. The authors also reported a 20% mismatch between the fitted and the observed temperatures, which they explained by a temperature gradient in the measurement cell.

A modified model for high pressures, assuming an effective temperature instead of the observed one, was tested in Ref. [20]. The measurements reported in Ref. [19] were completed in the same parameter space as reported in [21],

*Contact author: robin.groessle@kit.edu

†Contact author: geza.zsigmond@psi.ch

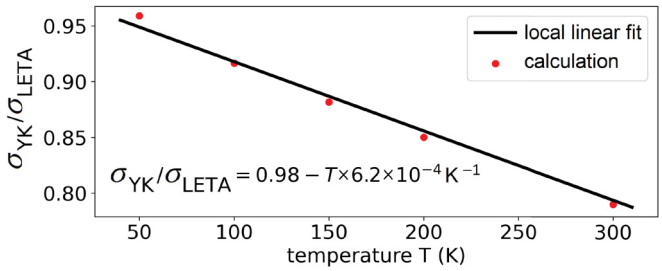

FIG. 1. Ratio of the UCN upscattering cross sections calculated from the YK and LETA models revealing the discrepancy between the temperature dependences, and a local linear fit approximation with its parameters.

in which the double-differential cross section of molecular hydrogen was measured at room temperature (RT) and could be fitted by using the YK model.

A significant time later, the total cross section of deuterium gas at 25 K was measured [22]. However, the YK model and a low-energy approximation model could not be distinguished at this single low temperature, thus it did not provide a full corroboration of the YK model. New gas measurements were performed at room temperature [23,24], where the authors scaled with $\sqrt{T}$ the 25 K value reported in Ref. [22] to an RT value. With simple reasoning, in the coordinate system of the molecules, the UCNs propagate with the mean velocity of the Maxwell-Boltzmann gas, $w \propto \sqrt{T}$, and the interaction rate σw is invariant to changing the coordinate system (see also Eq. (4) in Ref. [22]). This assumption of the low-energy low-temperature approximation (LETA) is oversimplified at higher D_2 gas temperatures. The LETA model is similar to the monoatomic gas model [25], however, it uses an effective scattering cross section neglecting rotations and spin-correlation effects. The YK theory shows an important deviation of the up-scattering cross section from a pure $\sqrt{T}$ dependence, which will be demonstrated experimentally in the present paper. Molecular vibrations are also included in the YK model, however, they are negligible in our experimental temperature range (vibration modes are populated only above 4000 K).

The total up-scattering cross section as a function of UCN energies can be calculated from Eqs. (A4) and (A5) in Ref. [16] by integrating over the solid angle and final energies. We obtained a temperature-dependence characteristic of the YK model. In Fig. 1 we plotted this dependence normalized with the LETA model, which only involves $T^{1/2}$ dependence. At low temperatures, below the linearity range shown, the two model predictions coincide, however, in the temperature range reaching above RT there is an important deviation. The YK model cross section is about 80% of that of LETA at RT.

III. EXPERIMENT

The experiment was designed to be sensitive to the difference between the monoatomic LETA and diatomic YK models, by measuring the transmission probability of UCNs passing through a gas as a function of pressure and temperature.

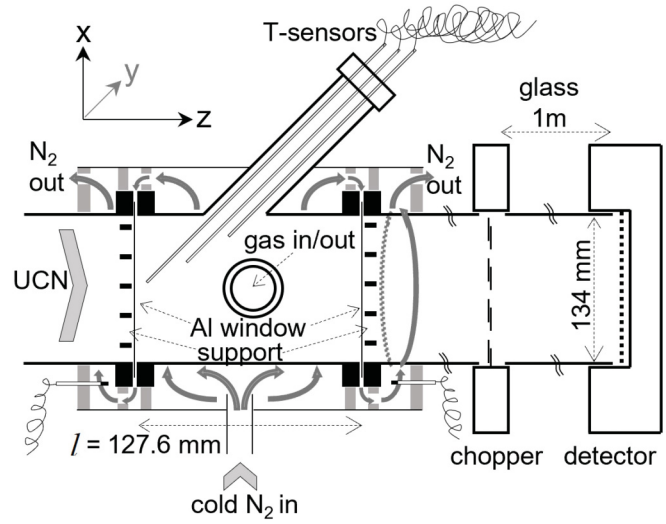

FIG. 2. The gas cell, chopper, and UCN detector (left to right, not to scale) in the standard TOF measurement. On the left side, the system was connected to the beam port West-1 of the UCN source.

A. Experimental setup

The experiment was conducted at beam port West-1 of the PSI UCN source, working with typically 8 s proton pulses on the target, which start UCN measurements lasting for 300 s until the next pulse [2–4]. Beam port South was used to monitor the UCN source stability. We employed glass tubes coated with nickel-molybdenum (NiMo) and polished stainless steel tubes as UCN guides. The gas cell was followed by a UCN chopper [26], a 1 m UCN guide, and a CASCADE UCN detector [27] (see Fig. 2).

The gas cell was connected with the beam port to the left and a chopper connecting via a 1 m UCN guide to the UCN detector as in a standard time-of-flight setup. This chopper was only used for calibration measurements, otherwise left permanently open, thus ensuring stable conditions for the transmission measurements.

The gas cell was sealed on both sides with 0.1 mm thick aluminum (AlMg3) windows to separate the gas volume from the vacuum in the UCN guides. This window was supported by stainless-steel grids that covered approximately 10% of the tubes cross section. The gas cell was made of stainless steel as a compromise between temperature stability and UCN guiding properties. Cooling was done with a cold gas system where the cold N_2 is guided first around the center of the cell and then in parallel to both ends. To achieve a good temperature equilibration with the windows, it was important that the cooling gas also cooled the stainless steel UCN guides connected to both sides of the cell. Calculations and finite element simulations showed that the highest temperature gradient was expected starting from the center of the window to the point where the cold N_2 gas is first reaching the cell. Therefore, we positioned several temperature sensors inside the gas volume, which were introduced from the top via a pipe at a 45-degree angle to the horizontal. Additional temperature sensors were used on the outside of the cell on both aluminum windows. The T sensors were calibrated beforehand with

liquid N_2 and distilled ice water. In the final analysis, a time- and position-averaged temperature value of the sensor readings was used. We also checked that the impact of temperature gradients on the final result is negligible compared to our main systematic uncertainty in the UCN dwell-time spectrum. Pressure sensors and the gas inlet were connected by a separate flange. For the pressure sensors a two point calibration was done at atmospheric pressure (using meteorologic reference data) and after evacuation with a two stage pump train (both with a systematic error smaller than 0.1%). We also made sure that there was no relevant effect of a temperature gradient on the pressure measurement.

B. Analysis concept

The survival probability for a single UCN with a dwell time t and mean lifetime τ inside the gas, when crossing the cell, is given by:

$$P = \exp(-t/\tau). \tag{1}$$

In an ideal system, the cell length, l, the velocity in axial direction, v_z, and the dwell time, t, are connected by the simple relation

$$t = l/v_z. \tag{2}$$

The lifetime of the UCNs inside the gas cell is given by:

$$\tau = (\rho\ \sigma\ v_\mathrm{n})^{-1} = \left(\frac{p}{k_\mathrm{B}\sqrt{T}}\,\epsilon\right)^{-1}, \tag{3}$$

where on the left-hand side, ρ is the number density of the gas molecules, v_n the neutron velocity and $\sigma = \sigma(T, v_\mathrm{n})$ the microscopic up-scattering cross section, which is inversely proportional to v_n in both YK and LETA models. On the right-hand side, we used the ideal gas law (valid at our experimental conditions), where p is the pressure in the cell, k_B the Boltzmann constant, and introduced the parameter ϵ defined as:

$$\epsilon = \frac{\sigma v_\mathrm{n}}{\sqrt{T}}. \tag{4}$$

We introduced this scaled cross section parameter to make the analysis sensitive to temperature dependence other than $\sqrt{T}$. In case that LETA is valid, ϵ would be independent of temperature. In case the YK model is valid, ϵ would depend linearly on T (in the range of interest), see Fig. 1.

Putting everything together gives a v_z-dependent model for the analysis of the transmission probability

$$P^{v_z}_\mathrm{gas}\left(l, p, T; \frac{\epsilon}{v_z}\right) = \exp\left(-\frac{lp}{k_\mathrm{B}\sqrt{T}}\,\frac{\epsilon}{v_z}\right), \tag{5}$$

where the first three arguments describe the experimental conditions for the gas.

The quantity ϵ is independent of temperature for monoatomic gases such as Ne and is temperature dependent for diatomic gases such as D_2. As indicated in Fig. 1 for D_2, the ratio of cross sections calculated with the YK and LETA models [thus also the ratio of the ϵ-s defined via Eq. (4)] can be approximated with a linear T-dependent fit function in the temperature range of interest (expecting discernible effects):

$$\epsilon(T) = \epsilon_0\ (\epsilon_a - \epsilon_T\ T), \tag{6}$$

where ϵ_0 represents the LETA approximation, and $\epsilon_a = 0.98 \pm 0.03$ and $\epsilon_T = (6.26 \pm 0.37) \times 10^{-4}\ \mathrm{K}^{-1}$. Besides the fit error, there is a ∼1 % error from the numerical uncertainty of the MC integration and ∼2 % from uncertainty in the input parameters such as the equilibrium distance of the nuclei. In total, we estimate the slope error to be below 6 %.

Other than in the theory, in the analysis of the measurements, one cannot disentangle ϵ_a from ϵ_0. However, we were looking for the temperature dependence additional to $\sqrt{T}$. The signature we were searching for was covered by ϵ_T. We thus set ϵ_a to the theoretically expected value of 0.98 valid in our temperature range of interest, and propagate its uncertainty into the final systematic error.

In our analysis, we used calibrated (see next section) values for l, p (0–1 bar), T (range for all gases: 110–365 K), and integrated Eq. (5) over the normalized neutron velocity distribution $f(v_z)$, which was extracted from the combined time-of-flight (TOF) measurements and D_2 calibration (see Fig. 3 and details below) to obtain a measurable transmission probability

$$P_\mathrm{gas}(l, p, T; \epsilon) = \int P^{v_z}_\mathrm{gas}\left(l, p, T; \frac{\epsilon}{v_z}\right) f(v_z)\mathrm{d}v_z, \tag{7}$$

where ϵ also involves the parameter ϵ_T. As explained later, to also consider unavoidable UCN storage effects in the cell,

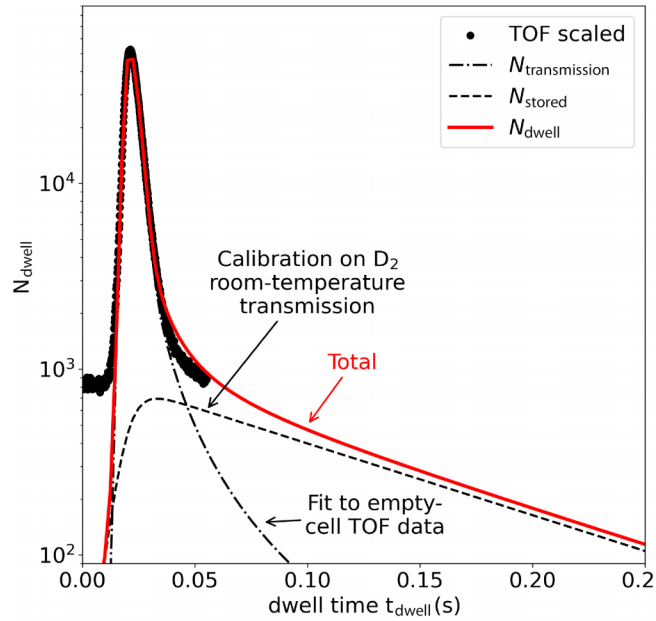

FIG. 3. The dwell-time spectrum of UCNs is composed of two parts. The time axis was scaled using the ratio of the effective length of the gas cell and the flight path. First part: the time-of-flight spectrum of raw neutron counts measured with an empty cell (black dots TOF scaled). The fit is denoted by $N_\mathrm{transmission}$. Second part: contribution of stored neutrons obtained from calibration to the RT data of D_2 denoted as N_stored. In the analysis we used the combined spectrum N_dwell (see text).

integration over the velocity distribution was replaced in the analysis by the equivalent integration over dwell time [see Eq. (1)].

We extensively investigated the measured data sets of two gases: neon (Ne) to serve as a test candidate for the LETA model and D_2 for the YK model. We checked whether ϵ_T is compatible with 0 in the case of Ne, and whether for D_2 it is compatible with the value $(6.26 \pm 0.37) \times 10^{-4}\,\mathrm{K}^{-1}$ from the theoretical Young-Koppel prediction.

As an additional check of systematics, mainly of the dwell-time spectrum, we also measured He, Ar, CF_4, Xe, and H_2 gases, but in a reduced p-T parameter space.

IV. SYSTEMATICS

To extract the transmission probability function P_{gas} from the measurements, four major systematic effects had to be taken into account:

(i) time variation of the UCN rate at the beam port [28],
(ii) faster neutrons during each beam pulse [2],
(iii) temperature-dependent transmission probability of the empty cell, mainly of the windows,
(iv) dwell time of UCNs in the gas cell.

A second CASCADE UCN detector (labeled here "B") on beam port South was used to monitor the UCN rate (measured with detector "A") at the West-1 beam port. Cutting the first 12 s after the start of the proton beam pulse eliminated the contribution of neutrons faster than UCN [26]. In this way the ratio R between the neutron count rates of the two detectors for the empty cell, was determined to be constant at the $<1\,\%$ level.

The temperature-dependent transmission behavior of the empty cell was taken care of by calibration, as described in the second section below, applying a temperature-dependent correction factor for the total transmission probability.

Taking these three systematic effects into account $P_{\mathrm{gas}}(T)$ can be written as:

$$P_{\mathrm{gas}}(T) = \frac{1}{R\,P_{\mathrm{window}}(T)}\,\frac{N_A(p,T)}{N_B}, \tag{8}$$

where N_A is the neutron count of the main detector and N_B is the neutron count of the monitoring detector for each proton beam pulse (both without the first 12 s). $P_{\mathrm{window}}(T)$ represents the temperature-dependent transmission probability of the empty cell and the UCN guides. The reference value R includes all other constant effects that influence the ratio between the number of counts in the detectors A and B.

A. Reference value of the setup with empty cell

The reference R was measured periodically after and before thermal annealing of the D_2 crystal [28,29] used for UCN production, for several UCN pulses with an empty cell. As the T dependence of the UCN guides and cell without test-gas was reproducible, it could be done at any temperature T_{ref} of the empty gas cell. However, most of the time it was measured at room temperature. The probability $P_{\mathrm{gas}}(T)$ with an empty cell must be per definition 1, therefore, R can be written as:

$$R = \frac{N_{A,\mathrm{ref}}(p=0,T_{\mathrm{ref}})}{P_{\mathrm{window}}(T_{\mathrm{ref}})}\,\frac{1}{N_{B,\mathrm{ref}}}. \tag{9}$$

B. Temperature dependence for the empty cell

For the empty cell we found a thermal correction function by fitting the transmission data:

$$P_{\mathrm{window}}(T) = \frac{C_T\,T + C_0}{C_0}, \tag{10}$$

where $C_T = (-1.73 \pm 0.03) \times 10^{-3} K^{-1}$ and $C_0 = 5.470 \pm 0.006$. Since it is impossible to disentangle the absolute transmission probability of the setup, the function was built in a way that it is 1 at 0 K. This is valid since the absolute scale will cancel out in P_{gas} with the absolute scale of $R(T_{\mathrm{ref}})$. The relevant part for this investigation is that the empty cell transmission changes with the temperature so that the transmission probability of the empty cell at around 100 K is about 6 % higher than at RT. This is plausible considering up scattering on phonons in the aluminum window causing a previously observed temperature dependence of the total UCN cross section on aluminum [30,31].

C. Pressure-induced change of cell length

The effective length of the gas cell changes with increasing pressure in the cell, due to a small bulging of the aluminum foils on the grid. The size of this effect was estimated via a measurement of the pressure change in the gas cell while on the other sides of the windows the pressure changed from 1 bar to 0 during pumping. At a starting pressure of 972.0 mbar a small but well-measurable drop to 964.5 mbar was observed and could be reproduced several times. This was interpreted by ideal gas law as a linear change in the average cell length of 0.8% from 0 bar to 1 bar with a linear dependence on the pressure.

Therefore, the effective mean length of the cell can be written as a function of pressure:

$$l = 127.6\,\mathrm{mm} + p \times 1.060\,\mathrm{mm/bar}. \tag{11}$$

This was in agreement with optical inspection and due to its small size a minor contribution in our analysis.

D. Calibration of the dwell-time spectrum

In our analysis the knowledge of the dwell-time distribution, $N(t_{\mathrm{dwell}})$, i.e., the time UCNs spend inside the gas cell, is needed. In an ideal setup, where the axial velocity of the neutrons, i.e., in the direction of the UCN guide axis, v_z, does not change over time, t_{dwell} can be derived from v_z:

$$t_{\mathrm{dwell}} = \frac{l_{\mathrm{cell}}}{v_z}, \tag{12}$$

or v_z can be measured via time-of-flight (TOF) from the chopper to the detector:

$$v_z = \frac{l_{\mathrm{TOF}}}{t_{\mathrm{TOF}}}. \tag{13}$$

The UCN time-of-flight distribution was first measured with the chopper installed after the gas cell as in a standard TOF measurement (Fig. 3). However, this setup is blind to neutrons that are stored for a considerable time within the gas cell due to diffuse reflections, which causes an additional systematic.

To determine the size of this effect, we made use of the RT subset of all D_2 transmission data measured with the chopper permanently open. First, from the TOF data taken with an empty cell, we performed an analytical parametrization of the main peak of the UCN spectrum. The profile can be described by a modified asymmetric Gaussian with a main peak around 0.025 s. This corresponds to a neutron velocity of 5.2 m/s (see TOF fit curve $N_{\text{transmission}}$ in Fig. 3). We checked for the impact of several factors such as the precise shape of the main peak or small deviations at the rising and falling flanks, and found those to be negligible in our case.

As the second step, to describe the part of stored neutrons that are not visible in the TOF data we added an exponential tail:

$$N_{\text{stored}} = a_{\text{storage}} \exp\left(-t_{\text{dwell}}/\tau_{\text{storage}}\right) \tag{14}$$

and on the left side a rising edge of the stored UCN curve which is described with a logistic growth function to emulate the filling of the system. The impact of the precise shape of the latter was found to be negligible. The final curve for the stored UCNs with calibrated parameters is shown as N_{stored} in Fig. 3. The calibration of the exponential constants was determined by a global fit of Eq. (7) to all room-temperature D_2-transmission data:

$$\begin{aligned} \tau_{\text{storage}} &= 112.5 \pm 8.0\,\text{ms}, \\ a_{\text{storage}} &= 968 \pm 115. \end{aligned} \tag{15}$$

Absolute amplitude values cancel out through later normalization, however, they are an indicator for statistical error estimation.

By this, we have a complete and calibrated description of the dwell-time spectrum. This was used in the analyses of all investigated gases at all temperatures and with both models (LETA and YK).

As an independent check of this exponential part, we rearranged the setup so that the chopper was placed before the cell. With this setup, we found a storage time constant of UCNs with around 92 ms, which is in reasonable agreement with the time constant we found through the calibration procedure with D_2 gas.

E. Systematic test with reference gases

To check our understanding of the dwell time, we measured UCN transmission of gases using He, Ne, Ar, CF_4, Xe as references, and derived the total neutron cross section for a given gas at a given temperature.

Again, accounting for the correct dwell-time spectrum including stored UCNs we found good agreement with the literature and calculated the values shown in Table I. We also obtained very good agreement with the measurements of Ne, Ar, Xe, CF4 in Ref. [23] at RT, the difference being smaller than the error bars. For reference, we considered 6.6 m/s UCN-velocity in order to compare to previous work [23] applying the same textbook equation (Eq. (11) in Ref. [23] from Ref. [32]) to convert from free atoms at rest to a Maxwell-Boltzmann gas. The values for the total cross section were obtained by fitting Eq. (7) to transmission data using the dwell-time spectrum from Fig. 3. The statistical uncertainty is extracted from the fit. The systematic uncertainty was calculated using maximum error propagation by fitting with minimum and maximum values derived from the uncertainties on τ_{storage} and a_{storage} [Eq. (15)].

By this, we find that for all investigated gases the systematic uncertainties dominate the statistical ones by at least one order of magnitude.

TABLE I. Measured total cross sections calculated for 6.6 m/s and at $T = 294.5$ K including statistical and systematic uncertainties. Most "literature" values were calculated from tabulated data [33]. Absorption data were all calculated from Ref. [33]. The CF_4 cross section is cited from Ref. [23]. The literature cross sections for D_2 and H_2 were calculated in this work by applying the YK model.

	this work			literature
species	σ barn	stat. $\pm$	syst. $\pm$	σ barn
He	185	1.13	17.0	164
Ne	255	0.566	23.7	214
Ar	287	1.74	24.9	264
Xe	8220	34.1	389	8063
CF_4	3450	1.87	141	3300
D_2	2626	18	157	2582
H_2	17400	49.7	969	18060

V. RESULTS AND DISCUSSION

The main transmission measurements were performed with gaseous D_2 (99.6% D_2 purity with a fraction of HD molecules of 0.4%, which has a negligible contribution compared to the main systematic effects discussed) and Ne in the pressure range from 0 bar to 1 bar, and from 110 K to 365 K. The pressure, p, and the temperature, T, of the gas are measured directly with sensors in each measurement.

In Eq. (5) the exponent of the transmission probability of a neutron is given as $(-\frac{lp}{k_B\sqrt{T}}\,\frac{\epsilon}{v_z})$, where the cell length, l, is dependent on the absolute pressure, p, according to Eq. (11). Consequently, the transmission can be plotted as a function of $(\frac{lp}{\sqrt{T}})$. By this choice, one expects a close-to-exponential dependence of the measured transmissions on $(\frac{lp}{\sqrt{T}})$, which also includes the broadening due to the dwell-time spectrum. These transmission profiles are seen in the top plots of Fig. 4 for D_2 gas and Fig. 5 for Ne.

The aforementioned spectral broadening would make calculating $\epsilon(T)$ directly as a function of transmission [by inverting Eq. (7)] to an arduous computational challenge. Thus we developed a feasible numerical fit alternative. In the data fit, we chose the transmission probability as the dependent variable, and the two independent variables were thus T and $(\frac{lp}{\sqrt{T}})$, which replaced p. The unknown quantity

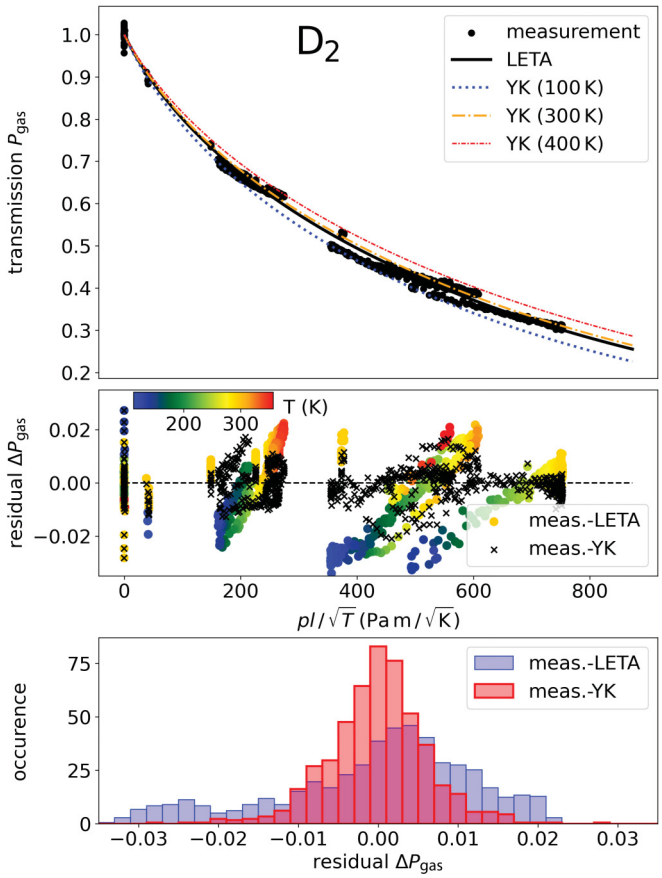

FIG. 4. Top: UCN transmission data (black dots) in D_2 gas as a function of $(\frac{lp}{\sqrt{T}})$ (at all measured T-s), and the best fits of the two alternative models with example values for the independent variable T in case of YK (blue = 100 K, yellow = 300 K, red = 400 K lines), and one line with LETA (black). Center: Point-by-point residuals of the YK and LETA model fits to the measured data, indicating smaller deviations for the YK model fit, showing data at all measured temperatures in a color scale. Bottom: Histograms of the above residuals showing a much narrower and symmetrical distribution for the case of the YK model.

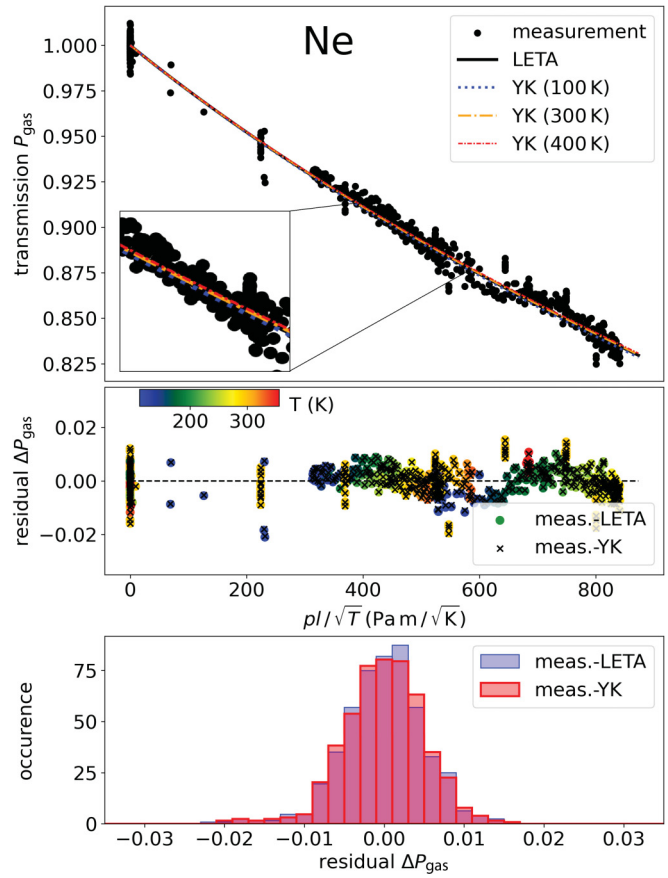

FIG. 5. Top: UCN transmission data (black dots) in Ne gas as a function of $(\frac{lp}{\sqrt{T}})$ (at all measured T-s), and the best fits of the two alternative models with example values for the independent variable T in the case of YK (blue = 100 K, yellow = 300 K, red = 400 K lines), and one line with LETA (black). The black and colored curves overlap (see insert), since no T dependence of ϵ was obtained from the Ne gas fit. Center: Residuals of the LETA and YK model fits to the measured data, here displaying all the measured temperatures in color scale. Bottom: Histograms of the above residuals.

given by the two-variable fit thus was ϵ. Therefore, for the LETA model a single-parameter (ϵ) fit and for the YK model a two-parameter (ϵ_0, ϵ_T) fit was performed. The latter additional parameter ϵ_T gave a small modulation to the exponential dependence, due to the additional T-dependent term, which served as the signature of the YK model. Our least-squares fit minimized the sum of the transmission residuals from all measurements for a given gas at different T and $(\frac{lp}{\sqrt{T}})$ values. The residuals were defined here as the difference between the measured UCN transmission and the one calculated via Eq. (7), taking into account that ϵ has the form as in Eq. (6).

In the top of Figs. 4 and 5, along with the measured transmissions, we also plotted the best fits with the two models for ϵ plugged into Eq. (7) (corresponding to YK and LETA): one with $\epsilon = \epsilon(T)$ [Eq. (6)] and one with ϵ independent of temperature. Since a full three-dimensional (3D) plot of this two-variable fit problem would be much more difficult to interpret, we visualized the theoretical fit in the plots using only three example values for the independent variable T (100 K, 300 K, and 400 K, not to be confounded with measured values).

In the case of the LETA model, the horizontal axis variable $(\frac{lp}{\sqrt{T}})$ is completely describing the $\sqrt{T}$ dependence. In the case of the YK model, an additional temperature dependence occurs via the T dependence of ϵ. Thus for different T-s, we obtain different slopes for the exponent in the transmission versus $(\frac{lp}{\sqrt{T}})$ corresponding to each $\epsilon(T)$. This results in splitting the exponential transmission curve into separate curves corresponding to the number of plotted temperatures. Exactly this splitting is the signal to distinguish between the LETA and YK models, as visualized in Fig. 4 for D_2 and in Fig. 5 for Ne. Here we plotted three lines (i.e., three 3D slices) for YK corresponding to three example values of the independent variable T enclosing the range of the measured temperatures.

In contrast to D_2, the Ne data fits with different temperatures shown in Fig. 5 converge with a slope in T compatible with zero, see also Table II, hence the fit involving Eq. (6) reproduces the LETA model.

TABLE II. Best model fit parameters for Ne and D_2 data with an additional parameter for a linear temperature dependence of the up-scattering cross section according to the YK model as shown in Eq. (6) and Fig. 1.

Species	ϵ_0 $\left(\frac{\text{barn } m/s}{K^{1/2}}\right)$	stat. ±	syst. ±	ϵ_T $10^{-6}/K$	stat. ±	syst. ±
Ne	100.6	1.0	11.0	54	38	10
D_2	1238.8	3.8	66	559	10	18

The best fit of the Ne data results in $\epsilon_T = (54 \pm 38 \pm 10) \times 10^{-6}\,\text{K}^{-1}$, which is about compatible with zero considering the uncertainties. For D_2 gas data the fit yielded $\epsilon_T = (559 \pm 10 \pm 6) \times 10^{-6}\,\text{K}^{-1}$, with very high significance in terms of uncertainty.

The central plots display the residuals for both model fits. No distinction between the models is visible in the Ne case, hence the parameter ϵ_T does not contribute. In the D_2 gas case, this is clearly different: the LETA model shows systematic deviations that vanish when using the YK model. The same is true in the histogram of residuals in the bottom plots in Figs. 4 and 5.

The fit results are summarized in Table II. As in the results for other gases (Table I), the uncertainties of ϵ_0 are for both gases, D_2 and Ne, dominated by the systematic contribution from N_{dwell}, whereas, for ϵ_T the uncertainties are dominated by statistics, as the latter is a relative parameter. The neutron counts per measurement point for both detectors were above 3×10^5. However, considering only pure neutron count rate statistics would neglect other effects, such as minor changes in the neutron spectrum due to slow changes in the neutron production efficiency of the source.

The cross check with Ne gas gives further confidence that in our current investigation, the function N_{dwell} fitted to the extended tail, which represents stored UCNs, is appropriate, even if improvable for measuring absolute cross sections with higher accuracy.

We interpret the large ϵ_T value in the case of D_2 as a clear demonstration of an additional T-dependent term in the YK model compared to the LETA model for monoatomic gases. Comparing this result to the theoretical prediction $\epsilon_T = (626 \pm 37) \times 10^{-6}\,\text{K}^{-1}$, and considering the measurement uncertainties and the unevenly distributed residuals (center plots in Figs. 4 and 5) hints towards yet unresolved systematic uncertainties in the measurements.

Returning to Table I, the absolute value of the D_2 total cross section for UCNs is given under "literature" as calculated by integrating Eqs. (A4) and (A5) in Ref. [16] and adding in a 2:1 ortho-para RT-equilibrium ratio. Our measured value for RT is smaller than reported in Ref. [23] by a factor of 1.2 of the quadratically combined error bars. In Fig. 6 we plotted the D_2 total cross section as a function of temperature extracted by applying the YK model to the measured data using the parameters in Table II. We also measured the total cross section of UCNs in H_2 gas. The data were analyzed by applying the Young-Koppel model, however, in a more limited temperature range (250–350 K) and thus with less sensitivity to the details of this model. The theoretical YK differential cross sections, Eqs. (29)–(30) in Ref. [16], for para- and ortho-hydrogen were integrated over final energy and solid angle, and added in a 1:3 para to ortho equilibrium ratio at RT. The measurement result for H_2 and the theoretical expectation are in very good agreement, see Table I, consistent within the systematic uncertainties. Our extracted value for RT is smaller than reported in [24] by a factor of 1.1 of the combined error bars.

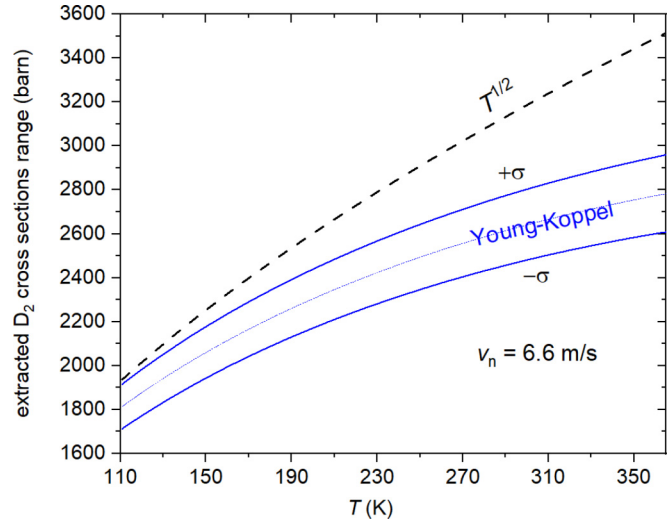

FIG. 6. Temperature dependence of the D_2 total cross section applying the YK model to all measured data. To emphasize the difference, the dashed line indicates the $\sqrt{T}$ dependence of the monoatomic approximation.

VI. SUMMARY AND CONCLUSION

We performed UCN transmission measurements in D_2 and other gases at temperatures between 110 K and 365 K. A comparison between the molecular deuterium and the monoatomic neon gas showed a clearly different temperature dependence of the total cross section. We analyzed our data using the Young-Koppel model and a low-energy low-temperature approximation. We interpret our best fit to the D_2 gas data as a strong confirmation for an additional temperature-dependent term due to spin correlations and rotational molecular states as described by the Young-Koppel model. This is an important confirmation of the YK theory and has implications for the understanding of deuterium-based ultracold neutron sources.

ACKNOWLEDGMENTS

We acknowledge the PSI proton accelerator operations section, many PSI support groups, and the BSQ group for the excellent operation of the UCN source. Excellent technical support by M. Meier is acknowledged. This work was supported by the Swiss National Science Foundation Projects No. 178951 and No. IZSEZ0_187982.

DATA AVAILABILITY

The data supporting this study's findings are available within the article.

[1] R. Golub, D. Richardson, and S. Lamoreaux, *Ultra-Cold Neutrons* (Adam Hilger, Bristol, 1991).

[2] G. Bison, B. Blau, M. Daum, L. Göltl, R. Henneck, K. Kirch, B. Lauss, D. Ries, P. Schmidt-Wellenburg, and G. Zsigmond, Eur. Phys. J. A **56**, 33 (2020).

[3] G. Bison, M. Daum, K. Kirch, B. Lauss, D. Ries, P. Schmidt-Wellenburg, and G. Zsigmond, Eur. Phys. J. A **58**, 103 (2022).

[4] B. Lauss and B. Blau, SciPost Phys. Proc. 004 (2021).

[5] C. Abel, S. Afach, N. J. Ayres, C. A. Baker, G. Ban, G. Bison, K. Bodek, V. Bondar, M. Burghoff, E. Chanel, Z. Chowdhuri, P.-J. Chiu, B. Clement, C. B. Crawford, M. Daum, S. Emmenegger, L. Ferraris-Bouchez, M. Fertl, P. Flaux, B. Franke *et al.*, Phys. Rev. Lett. **124**, 081803 (2020).

[6] N. J. Ayres, G. Ban, L. Bienstman, G. Bison, K. Bodek, V. Bondar, T. Bouillaud, E. Chanel, J. Chen, P. J. Chiu, B. Clement, C. Crawford, M. Daum, B. Dechenaux, C. B. Doorenbos, S. Emmenegger, L. Ferraris-Bouchez, M. Fertl, A. Fratangelo, P. Flaux *et al.*, Eur. Phys. J. C **81**, 512 (2021).

[7] J. Auler, M. Engler, K. Franz, J. Kahlenberg, J. Karch, N. Pfeifer, K. Ross, C.-F. Strid, N. Yazdandoost, E. Adamek, S. Kaufmann, C. Schmidt, P. Blümler, M. Fertl, W. Heil, and D. Ries, J. Phys. G: Nucl. Part. Phys. **51**, 115103 (2024).

[8] J. Schwinger and E. Teller, Phys. Rev. **52**, 286 (1937).

[9] M. Hamermesh and J. Schwinger in, Phys. Rev. **55**, 671 (1939).

[10] M. Hamermesh and J. Schwinger, Phys. Rev. **69**, 145 (1946).

[11] K. B. Grammer, R. Alarcon, L. Barrón-Palos, D. Blyth, J. D. Bowman, J. Calarco, C. Crawford, K. Craycraft, D. Evans, N. Fomin, J. Fry, M. Gericke, R. C. Gillis, G. L. Greene, J. Hamblen, C. Hayes, S. Kucuker, R. Mahurin, M. Maldonado-Velázquez, E. Martin *et al.*, Phys. Rev. B **91**, 180301(R) (2015).

[12] D. Blyth *et al.* (NPDGamma Collaboration), Phys. Rev. Lett. **121**, 242002 (2018).

[13] L. Zanini, E. Dian, D. D. DiJulio, B. Folsom, E. B. Klinkby, Z. Kokai, J. I. Marquez Damian, B. Rataj, N. Rizzi, V. Santoro, M. Strothmann, A. Takibayev, R. Wagner, and O. Zimmer, J. Neutron Res. **24**, 77 (2022).

[14] D. D. Dijulio, J. I. M. Damian, M. Bernasconi, D. Campi, G. Gorini, T. Kittelmann, E. Klinkby, G. Muhrer, K. Ramic, N. Rizzi, and V. Santoro, EPJ Web of Conf. **284**, 17013 (2023).

[15] D. Ries, The source for utracold neutrons at the Paul Scherrer Institute-Characterisation, optimisation, and international comparison, Ph.D. thesis, ETH Zürich, 2016.

[16] J. Young and J. Koppel, Phys. Rev. **135**, A603 (1964).

[17] J. Koppel and J. Young, Nukleonik **8**, 40 (1969).

[18] G. Squires and A. Stewart, Proc. R. Soc. London A **230**, 19 (1955).

[19] K. Herwig and R. Simmons, Mol. Phys. **75**, 1393 (1992).

[20] G. Corradi, M. Celli, N. Rhodes, A. K. Soper, and M. Zoppi, Phys. B: Condens. Matter **350**, E1063 (2004).

[21] E. Guarini, A. Orecchini, F. Formisano, F. Demmel, C. Petrillo, F. Sacchetti, U. Bafile, and F. Barocchi, J. Phys.: Condens. Matter **17**, 7895 (2005).

[22] F. Atchison, B. van den Brandt, T. Brys, M. Daum, P. Fierlinger, P. Hautle, R. Henneck, K. Kirch, J. Kohlbrecher, G. Kuhne, J. A. Konter, A. Pichlmaier, A. Wokaun, K. Bodek, M. Kasprzak, M. Kuzniak, P. Geltenbort, M. Giersch, J. Zmeskal, M. Hino *et al.*, Phys. Rev. Lett. **94**, 212502 (2005).

[23] S. J. Seestrom, E. R. Adamek, D. Barlow, L. J. Broussard, N. B. Callahan, S. M. Clayton, C. Cude-Woods, S. Currie, E. B. Dees, W. Fox, P. Geltenbort, K. P. Hickerson, A. T. Holley, C. Y. Liu, M. Makela, J. Medina, D. J. Morley, C. L. Morris, J. Ramsey, A. Roberts *et al.*, Phys. Rev. C **92**, 065501 (2015).

[24] S. J. Seestrom, E. R. Adamek, D. Barlow, M. Blatnik, L. J. Broussard, N. B. Callahan, S. M. Clayton, C. Cude-Woods, S. Currie, E. B. Dees, W. Fox, M. Hoffbauer, K. P. Hickerson, A. T. Holley, C. Y. Liu, M. Makela, J. Medina, D. J. Morley, C. L. Morris, R. W. Pattie, Jr. *et al.*, Phys. Rev. C **95**, 015501 (2017).

[25] A. C. Zemach and R. J. Glauber, Phys. Rev. **101**, 118 (1956).

[26] G. Bison, W. Chen, P.-J. Chiu, M. Daum, C. B. Doorenbos, K. Kirch, V. Kletzl, B. Lauss, D. Pais, I. Rienäcker, P. Schmidt-Wellenburg, and G. Zsigmond, Eur. Phys. J. A **59**, 215 (2023).

[27] CDT GmbH (2024), www.n-cdt.com.

[28] A. Anghel, T. L. Bailey, G. Bison, B. Blau, L. J. Broussard, S. M. Clayton, C. Cude-Woods, M. Daum, A. Hawari, N. Hild, P. Huffman, T. M. Ito, K. Kirch, E. Korobkina, B. Lauss, K. Leung, E. M. Lutz, M. Makela, G. Medlin, C. L. Morris *et al.*, Eur. Phys. J. A **54**, 148 (2018).

[29] I. Rienäcker, Improving ultracold neutron yields and the search for mirror neutrons at the PSI UCN source, Ph.D. thesis, ETH Zürich, 2022.

[30] A. Steyerl, Transmissionsmessungen mit ultrakalten Neutronen, Ph.D. thesis, Technische Universität München, 1971.

[31] A. Steyerl and H. Vonach, Z. Phys. **250**, 166 (1972).

[32] V. Turchin, *Slow Neutrons* (Israel Program for ScientificTranslations, Jerusalem, 1965).

[33] V. F. Sears, Neutron News **3**, 26 (1992).